$Nb_3O_{10}\cdot 0.5H_2O$, acts as solid acid and reacts with organic bases such as 1,n-alkyldiamines to give intercalation compounds. These intercalation reactions are relatively facile even though the strontium niobate layers are thick and rigid compared to the layers of clay minerals or other oxides known to undergo intercalation reaction. However, the main shortcoming of these organic intercalation compounds for application as catalysts in high temperature is their insufficient thermal stability. We are now investigating the pillaring chemistry of these Dion series oxides using Keggin's ion, $[Al_{13}O_4(OH)_{24}(H_2O)_{12}]^{7+}$.

References

1. Lal, M.; Howe, A. T. *J. Sol. State Chem.* **1984**, *51*, 355.
2. Lichard, M.; Brohan, L.; Tournoux, M. *J. Sol. State Chem.* **1994**, *112*, 345.
3. Wells, A. F. *Structural Inorganic Chemistry*; Clarendon Press: Oxford; 1984 p 602.
4. Dion, M.; Ganne, M.; Tournoux, M. *Mat. Res. Bull.* **1981**, *16*, 1429.
5. Jacobson, A. J.; Johnson, J. W.; Lewandowski, J. T. *Inorg. Chem.* **1985**, *24*, 3727.
6. Gopalakrishnan, J.; Bhat, V. *Mat. Res. Bull.* **1987**, *22*, 413.
7. Gopalakrishnan, J.; Bhat, V. *Inorg. Chem.* **1987**, *26*, 4299.
8. Subramanian, M. A.; Gopalakrishnan, J.; Sleight, A. W. *Mat. Res. Bull.* **1988**, *23*, 837.
9. Thomas, J. M. *J. Chem. Comm. Daton Trans* **1991**, 555.
10. Yoshimura, J.; Ebina, Y.; Kondo, J.; Domen, K.; Tanaka, A. *J. Phys. Chem.* **1993**, *97*, 1970.
11. Anderson, M. W.; Klinowski, J. *Inorg. Chem.* **1990**, *29*, 3260.
12. Tang, X.; Xu, W. Q.; Shen, Y. F.; Suib, S. L. *Chem. Mater.* **1995**, *7*, 102.
13. Jacobson, A. J.; Lewandowski, J. T.; Johnson, J. W. *J. Less-Common Met.* **1986**, *156*, 137.
14. Cheng, S.; Wang, T. C. *Inorg. Chem.* **1989**, *28*, 1283.
15. Jacobson, A. J.; Johnson, J. W.; Lewandowski, J. T. *Mat. Res. Bull.* **1987**, *22*, 45.
16. England, W. A.; Goodenough, J. B.; Wiseman, P. J. *J. Solid State Chem.* **1983**, *49*, 289.
17. Kumada, N.; Takeshita, M.; Muto, F.; Kinomura, N. *Mat. Res. Bull.* **1988**, *23*, 1050.

Molecular Dynamics Simulation of Liquid Alkanes. I. Thermodynamics and Structures of Normal Alkanes: *n*-butane to *n*-heptadecane

Song Hi Lee*, Hong Lee, Hyungsuk Pak†, and Jayendran C. Rasaiah‡

Department of Chemistry, Kyungsung University, Pusan 608-736, Korea
†Department of Chemistry, Seoul National University, Seoul 151-740, Korea
‡Department of Chemistry, University of Maine, Orono, Maine 04469, USA

Received April 29, 1996

We present results of molecular dynamic (MD) simulations for the thermodynamic and structural properties of liquid *n*-alkanes, from *n*-butane to *n*-heptadecane, using three different models I-III. Two of the three classes of models are collapsed atomic models while the third class is an atomistically detailed model. Model I is the original Ryckaert and Bellemans' collapsed atomic model [*Discuss. Faraday Soc.* **1978**, *66*, 95] and model II is the expanded collapsed model which includes C-C bond stretching and C-C-C bond angle bending potentials in addition to Lennard-Jones and torsional potentials of model I. In model III all the carbon and hydrogen atoms in the monomeric units are represented explicitly for the alkane molecules. Excellent agreement of the results of our MD simulations of model I for *n*-butane with those of Edberg *et al.* [*J. Chem. Phys.* **1986**, *84*, 6933], who used a different algorithm confirms the validity of our algorithms for MD simulations of model II for 14 liquid *n*-alkanes and of models I and III for liquid *n*-butane, *n*-decane, and *n*-heptadecane. The thermodynamic and structural properties of models I and II are very similar to each other and the thermodynamic properties of model III for the three *n*-alkanes are not much different from those of models I and II. However, the structural properties of model III are very different from those of models I and II as observed by comparing the radial distribution functions, the average end-to-end distances and the root-mean-squared radii of gyrations.

Introduction

Liquid alkanes exhibit a vast variety of interesting physical properties which follow a pattern starting with methane that is consistent with the alkane structure.[1] An alkane molecule is held together entirely by covalent bonds, which either join two atoms of the same kind and hence are non-polar, or they join two atoms that differ a little in electronegativity

and hence are only slightly polar. The forces holding nonpolar molecules together (van der Waals force) are weak and of very short range; they act only between the portions of different molecules that are in close contact, that is, between the contiguous surfaces of molecules. Therefore one would expect that within a family, the larger the molecule, and hence the larger its surface area, the stronger the intermolecular forces. The boiling points and melting points of liquid alkanes thus rise as the number of carbon atoms increases. The processes of boiling and melting require overcoming the intermolecular forces of the liquid and solid respectively.

Computer simulation methods of liquid systems at the molecular level have become an important tool for the study of these systems, and provide primary information about their structural and dynamic properties. In order to study the dynamic properties of an assembly of chain molecules, it is convenient to employ the method of molecular dynamics (MD) simulation which has been extensively used in recent years to treat even complicated systems which have many internal degrees of freedom. In this paper we undertake an MD study of different models for the alkanes.

Various models, at many levels of detail, for liquid alkanes and polymers have been designed and used. The coarsest is the bead-and-spring model in which about 20 monomeric units of the polymer chain are lumped together as a single spherical unit (bead) and the net intramolecular interaction between beads is modeled by a spring interaction.[2] There are several variations of this basic model, including the case of finitely extensible non-linear elastic (FENE) interactions between beads.[3~6]

In 1978 an MD simulation study of *n*-alkanes by Ryckaert and Bellemans[7] was performed using the SHAKE algorithm and the matrix method to implement holonomic constraints in simulations of complex molecules.[8] The alkane model used by them is the so-called collapsed atomic model; monomeric units (methylene or methyl) are typically treated as single spheres with a standard 12-6 Lennard-Jones (LJ) potential between the spheres. The distance between neighboring spheres is fixed at 1.53 A and the bond angles are also fixed at 109.47 degrees. In addition to the LJ potential, a C-C-C-C torsional rotational potential is also included which models the missing hydrogen atoms in molecular conformation.[7,9] The main benefit of this model is to reduce considerably the amount of computing time by reducing the number of interaction sites. We shall refer to this model as model I in this work. Several MD simulation studies of *n*-alkanes using this model have been reported.[10~15]

Edberg, Evans, and Morriss developed a new algorithm (called EEM), which uses a fast, exact solution for constraint forces and a new procedure to correct for accumulating numerical errors, in MD simulations of liquid *n*-butane and *n*-decane molecules.[10] Baranyai and Evans have further developed a simple way of modifying the EEM method so that numerical drift in holonomic constraints can be treated in a simple non-iterative fashion and have applied this algorithm in the MD simulations of liquid benzene and naphthalene.[11] Evans and his coworkers have also used non-equilibrium molecular dynamics (NEMD) to study the rheological behavior of liquid alkanes such as butane, decane, eicosane, tridecane, and 5-butyl nonane under homogenous shear in NVT (canonical) and NpT (isobaric-isothermal) ensembles,[12~15] using the original Ryckaert-Bellemans (RB) collapsed atomic model.[7,9,10] In their later works,[13~15] they replaced the LJ potentials by potentials truncated at its minimum $r=2^{1/6}\sigma$, and shifted so that it is zero at the point of truncation. This potential is often referred to as the Weeks-Chandler-Andersen (WCA) prescription.[16,17]

Rowley and Ely adopted the original RB model to study the isomeric effects on the viscosity of butanes (normal and isomeric butanes)[18] by NEMD simulations using the NVT algorithm developed by Edberg *et al.* (EEM).[10] Following that, they continued the NEMD simulations to investigate the isomeric effects on the viscosity of models for *n*-hexane, cyclohexane, and benzene.[19]

Chynoweth and his coworkers have expanded the RB model by accounting for intramolecular interactions between the RB blobs.[20] For this, bond stretching and bond angle bending potentials were added to the original torsional rotational, and intra and inter LJ potentials of the RB model. They used this model for the rheological properties of liquid *n*-butane[21] and liquid *n*-hexadecane.[22] We shall refer to this model as model II. More refined collapsed atomic models for alkanes have been described by Toxvaerd.[23]

The most detailed model for alkane molecules and polymers is the so-called atomistically detailed model in which all the atoms i.e carbon (C) and hydrogen (H) atoms in the monomeric units, are treated explicitly. Muller-Plathe and his coworkers used this model in MD simulation studies of penetrant diffusion[24~28] -the diffusion of low molecular weight species in a polymer melt and showed that models for polymer melts analogous to the RB collapsed model and the atomistically detailed model differ by two orders of magnitude in the predicted penetrant diffusion rates. They also pointed out that only the atomistically detailed model agreed well with experimental data. We shall refer to this model as model III. The use of atomistically detailed models to describe polymer melts is reviewed by Gusev *et al.*[29]

More recently, Lee and Cummings[30] have reported an NEMD simulations of planar Couette flow of normal (*n*-butane) and isomeric butane (*i*-butane) molecules using three different models-the above referred models I, II, and III. They found that the collapsed atomic models predict the viscosity of *n*-butane quite well in general agreement with previous workers[12,18,20] but if these models are applied to the isomer, the viscosity is underpredicted. They also found that their atomistically detailed model does not yield quantitative agreement with the viscosity of either the *n*-butane or its isomer. However this model have the one positive feature that the calculated viscosity of i-butane is higher than that of *n*-butane (branching increases the viscosity) as observed experimentally. The results suggest that the inclusion of H atoms may be important in correctly predicting the effect of molecular structure on physical properties of liquid alkanes.

In this paper, we begin a series of molecular dynamics simulation studies to investigate the thermodynamic and structural properties of liquid *n*-alkanes, *n*-butane to *n*-heptadecane, using the above referred models. Further studies also include dynamic properties of liquid *n*-alkanes, the inve-

stigation of the corresponding properties of branched-chain alkanes, and analyses of segmental motions of C-C backbone chains in long chain alkanes.

The paper is organized as follows. Section II contains a brief description of molecular models and MD simulation methods followed by Sec. III which presents the results of our simulations and Sec. IV where our conclusions are summarized.

Molecular Dynamics Simulations and Molecular Models

In the present study, we have selected 14 systems for MD simulations using the three different models for liquid *n*-alkanes, from *n*-butane to *n*-heptadecane, all at 293.15 K except for a minor change in temperature to 291.0 K for *n*-butane and to 296.0 K for *n*-heptadecane. Each simulation was carried out in the NVT ensemble; the density and hence the length of cubic simulation box were fixed and listed in Table 1. The usual periodic boundary condition in the x-, y-, and z-directions and minimum image convention for pair potential were applied. A spherical cut-off of radius $R_c=2.5\ \sigma$, where σ is the LJ parameter, was employed for all the pair interactions. Gaussian isokinetics[31] was used to keep the temperature of the system constant.

The original RB collapsed atomic model (model I). Monomeric units are treated as single spheres with masses given in Table 1. They interact through an LJ potential between the spheres in different molecules and between the spheres more than three apart on the same molecule. The C-C-C-C torsional rotational potential is given by the original Ryckaert-Bellemans form[7]:

$$V(\phi)=c_0+c_1\cos\phi+c_2\cos^2\phi+c_3\cos^3\phi+c_4\cos^4\phi+c_5\cos^5\phi \quad (1)$$

where ϕ is the C-C-C-C dihedral angle. The LJ parameters and c's are listed in Table 2.

For this model, only three systems, *n*-butane, *n*-decane, and *n*-heptadecane, were simulated and the results were compared with those of other models. This was sufficient since all 14 systems are simulated for the expanded model

Table 1. MD simulation parameters for models of liquid *n*-alkanes

n-alkane	number of molecules	mass of site* (g/mole)	temperature (K)	density (g/cc)	length of box (nm)
n-C_4H_{10}	64	14.531	291.0	0.583	2.1964
n-C_5H_{12}	64	14.430	293.15	0.626	2.3052
n-C_6H_{14}	64	14.363	293.15	0.659	2.4043
n-C_7H_{16}	64	14.315	293.15	0.684	2.4970
n-C_8H_{18}	27	14.279	293.15	0.703	1.9386
n-C_9H_{20}	27	14.251	293.15	0.718	2.0008
n-$C_{10}H_{22}$	27	14.228	293.15	0.730	2.0598
n-$C_{11}H_{24}$	27	14.210	293.15	0.740	2.1157
n-$C_{12}H_{26}$	27	14.195	293.15	0.749	2.1685
n-$C_{13}H_{28}$	27	14.182	293.15	0.757	2.2185
n-$C_{14}H_{30}$	27	14.171	293.15	0.764	2.2665
n-$C_{15}H_{32}$	27	14.161	293.15	0.769	2.3136
n-$C_{16}H_{34}$	27	14.153	293.15	0.775	2.3574
n-$C_{17}H_{36}$	27	14.145	296.0	0.782	2.3979

*For model III, the masses of carbon and hydrogen atoms are used.

Table 2. Potential parameters for three different models of liquid *n*-alkanes

Model I	LJ parameters	σ(nm)	ε(kJ/mol)				
	C-C	0.3923	0.5986				
	torsional[a]	c_o(kJ/mol)	c_1	c_2	c_3	c_4	c_5
	C-C-C-C	9.279	12.136	−13.120	−3.060	26.240	−31.495
Model II	bond stretching	r_e(nm)	K_r(kJ/mol·nm^2)				
	C-C	0.153	132600				
	bond angle bending	θ_e(deg)	K_1(kJ/mol·deg^2)	K_2(kJ/mol·deg^3)			
	C-C-C	109.47	0.05021	0.000482			
Model III	LJ parameters	σ(nm)[b]		ε(kJ/mol)[b]			
	C-C	0.33665 (0.33665) [0.3207]		0.40561 (0.40561) [0.3519]			
	C-H	0.27983 (0.30561) [0.2763]		0.17219 (0.17219) [0.3345]			
	H-H	0.22300 (0.27457) [0.2318]		0.07310 (0.07310) [0.3180]			
	bond stretching	r_e(nm)		K_r(kJ/mol·nm^2)			
	C-C	0.153		210000			
	C-H	0.110		147000			
	bond angle bending	θ_e(deg)		K_1(kJ/mol·deg^2)			
	C-C-C	111.0		0.07346			
	C-C-H	109.5		0.05588			
	H-C-H	107.9		0.04667			
	torsional K_3(kJ/mol)						
	C-C-C-H	11.72					

[a]The same tortional parameters are used for models II and III. [b]( ) are used in Ref. 30 and [ ] are Muller-Plathe *et al*'s.

(model II) and the results of these two collapsed models are very similar. The MD simulations were performed using the Verlet algorithm[32] for the time integration of the equations of motion with a time step of 0.001 ps and the RATTLE algorithm[33] for the bond length and bond angle constraints. MD runs of at least 200,000 time steps each were needed for the liquid alkane system to reach equilibrium. The equilibrium properties were then averaged over 10 blocks of 10,000 time steps (10 ps) for a total of 100,000 time steps (100 ps).

The expanded collapsed atomic model (model II). This model includes the C-C bond stretching and C-C-C bond angle bending potentials in addition to the LJ and torsional potentials of model I:

$$V_b(r_{ij})=K_o\ (r_{ij}-r_e)^2 \tag{2}$$

$$V_a(\theta)=K_1\ (\theta-\theta_e)^2-K_2\ (\theta-\theta_e)^3 \tag{3}$$

The equilibrium bond length (r_e) and bond angle (θ_e), and the force constants (K_o, K_1, and K_2) are used by Chynoweth *et al.*[20~22] which are originally provided by the work of White and Boville,[34] and are given in Table 2.

For the integration over time, we adopted Gear's fifth-order predictor-corrector algorithm[35] with a time step of 0.0005 ps for all the *n*-alkanes. The equilibrated configurations of model I were used for the initial configurations for model II of *n*-butane, *n*-decane, and *n*-heptadecane. Other molecular configurations were prepared by adding a monomeric unit to an end of the configuration, one by one, after a full equilibration. A total of 100,000 or 150,000 time steps was simulated each for the average and the configurations of molecules were stored every 10 time steps for further analysis.

The atomistically detailed model (model III). The explicit presence of H atoms in the alkane molecule increases the number of interactions in inter and intra LJ potentials between H and H and between C and H atoms, as well as introducing C-H bond stretching, C-C-H and H-C-H bond angle bending, and also terminal C-C-C-H potentials. The bond stretching potential is of the same form as Eq. (2) but the bond angle bending potential has the form of Eq. (2) rather than Eq. (3). The terminal C-C-C-H torsional potential has a different form

$$V(\phi)=K_3\ (1-4\cos^3\phi+3\cos\phi) \tag{4}$$

from the C-C-C-C of Eq. (1). Here ϕ is the C-C-C-H dihedral angle and the potential parameters are listed in Table 2.

The Gear's fifth-order predictor-corrector algorithm[35] was also used with a time step of 0.00033333 ps. Also only three systems - *n*-butane, *n*-decane, and *n*-heptadecane - were simulated because of enormous computing times required. For example, to equilibrate the system of *n*-heptadecane, a configuration at a low density and high temperature was started, equilibrated, and then approached to the final state, which required approximately 1,000,000 time steps. The equilibrium properties were then averaged for a total of 150,000 time steps (50 ps).

In an NEMD simulation study of the isomeric effect on the viscosity of butanes using model III, Lee *et al.*[30] initially used the potential parameters developed by Muller-Plathe *et al.* for polyisobutylene[28] (shown in Table 2) except for the C-C-C-C torsional potential parameters. The NEMD results for *n*-butane and i-butane with these potential parameters

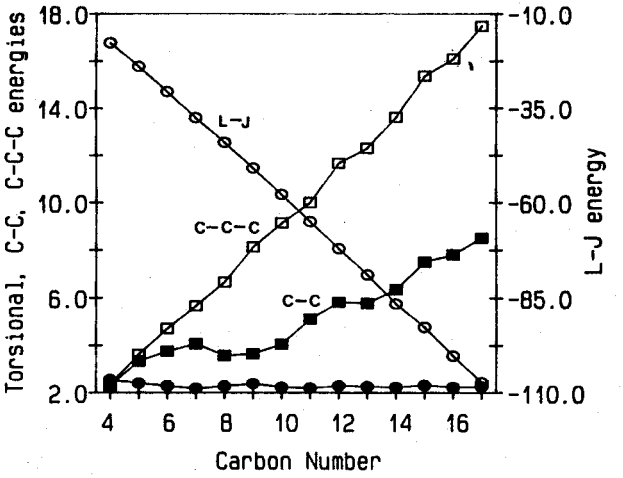

Figure 1. C-C-C-C torsional energy, C-C bond stretching energy, C-C-C bond angle bending energy, and LJ energy of model II for liquid *n*-alkanes as a function of carbon number.

deviated strongly from experiment. The calculated pressure was approximately −1000 atm in the absence of shear at a density of 0.583 g/cc and temperature of 291.0 K and under a homogeneous shear, the calculated density profiles showed a density inhomogeneity as shown in Figure 1 of Ref. 30. In NpT ensemble simulation at a pressure of 1 atm and temperature of 291.0 K, the density in the absence of shear was found to be 0.722 g/cc, much higher than the expected value of 0.583 g/cc.

In the MD simulation study of *n*-alkane tricosane by Ryckaert *et al.*,[36] a flexible-chain model was used in which the hydrogen atoms are incorporated explicitly, and the C-C and C-H bond lengths, and the H-H distances are constrained as constants. The intermolecular potential between atoms consists of "exp-6" interactions. Lee *et al.*[30] inferred LJ parameters from the exp-6 parameters by keeping the position of the potential minimum unchanged. The resulting potentials are in good agreement with the original exp-6 potentials, but the set of LJ parameters whichg do not follow the Lorentz-Berthelot mixing rule since the for H atoms is slightly too large, was further modified by changing the LJ parameters for H atom to comply with the mixing rule. The final LJ parameters used for their work[30] are given in Table 2. However, the calculated pressures of *n*-butane and i-butane using these parameters were very high (about 1000 atm), similar to those of model I.

We have further modified the LJ parameter for H atom to obtain a reasonable pressure of *n*-butane for model III by comparing the MD calculated pressures for various sets of for H atom. The final LJ parameters are listed in Table 2.

Results and Discussion

In this section we analyze the results of our MD simulations; the principal thermodynamic and structural properties are considered separately.

Thermodynamic properties. Thermodynamic properties of model I for liquid *n*-butane, *n*-decane, and *n*-heptade-

Table 3. Thermodynamic properties of model I for liquid *n*-butane, *n*-decane, and *n*-heptadecane

properties	*n*-butane	*n*-decane	*n*-heptadecane
molecular temperature (K)	291.0± 0.1	293.15± 0.18	296.0± 0.1
atomic temperature (K)	279.3± 1.8	271.24± 8.78	106.1± 1.9
pressure (atm)	53.4± 26.3	−111.9± 78.1	−254.2± 54.7
total C-C LJ energy (kJ/mol)	−17.73± 0.04	−58.62± 0.19	−108.50± 0.60
inter C-C LJ energy	−17.73± 0.04	−53.79± 0.17	−96.39± 0.47
intra C-C LJ energy	–	−4.83± 0.16	−12.11± 0.43
C-C-C-C torsional enrgy	2.507± 0.118	2.210± 0.127	2.306± 0.056
average % of C-C-C-C *trans*	60.02± 3.89	71.66± 4.60[a]	69.81± 4.36[a]
total barrier crossings T-G	293/100,000	394/100,000	803/100,000
G-T	300/100,000	398/100,000	834/100,000
av. end-to-end distance (nm)	0.3490± 0.0034	0.9330± 0.0067	1.4458± 0.0329
rms radius of gyration	0.1410± 0.0006	0.3215± 0.0015	0.4959± 0.0083

[a]average of 7 dihedral states. [a]average of 14 dihedral states.

Table 4. Thermodynamic properties of model II for liquid *n*-butane, *n*-decane, and *n*-heptadecane

properties	*n*-butane	*n*-decane	*n*-heptadecane
molecular temperature (K)	291.0± 0.2	293.15± 0.09	296.0± 0.2
atomic temperature (K)	249.9± 1.8	234.31± 6.20	243.7± 9.9
pressure (atm)	49.5± 62.3	9.3± 119.8	−292.7± 114.6
total C-C LJ energy (kJ/mol)	−17.66± 0.11	−57.63± 0.41	−107.26± 0.48
inter C-C LJ energy	−17.66± 0.11	−52.96± 0.38	−95.96± 0.44
intra C-C LJ energy	–	−4.87± 0.31	−11.32± 0.40
C-C-C-C torsional enrgy	2.560± 0.201	2.241± 0.115	2.271± 0.060
C-C stretching energy	2.305± 0.212	4.059± 0.164	8.670± 0.344
C-C-C angle bending energy	2.372± 0.172	9.153± 0.308	17.61± 0.19
average % of C-C-C-C *trans*	64.12± 0.40	74.69± 2.66[a]	75.54± 4.89[b]
total barrier crossings T-G	252/100,000	399/100,000	849/100,000
G-T	248/100,000	402/100,000	854/100,000
av. end-to-end distance (nm)	0.3519± 0.0037	0.9375± 0.0263	1.5210± 0.0218
rms radius of gyration	0.1414± 0.0006	0.3235± 0.0048	0.5163± 0.0034

[a]average of 7 dihedral states. [b]average of 14 dihedral states.

cane are listed in Table 3. The results for *n*-butane compare well with those of Edberg *et al.*[10] at the same MD simulation point. The agreement is excellent with respect to the C-C LJ energy (−17.73/−17.60), the average % of C-C-C-C *trans* (60.02/60.6), the average C-C-C-C torsional energy per dihedral state (2.507/2.762), and the barrier crossing rate (transitions/simulation time(ps)/number of molecules=0.046/0.045), even though the MD simulation algorithms are different. The only difference is the calculated pressure (47.7/428).

However, the MD simulation state points are different for *n*-decane -a density of 0.730 g/cc and temperature of 293.15 K for this work and 0.630 g/cc and 481 K respectively for Ref. 10. The denser and the lower the temperature of the system, the lower the total C-C LJ energy (−58.62/−44.17), and average C-C-C-C torsional energy per dihedral state (2.210/3.928), This is also accompanied by a larger average end-to-end distance (0.9330/0.8768) and root-mean-squared radius of gyration (0.3215/0.3101), which indicates an increase in the average C-C-C-C *trans* configuration as the system becomes denser and cooler. The most interesting result is that the inter C-C LJ energies are exactly the same (−4.83/−4.82).

In the case of *n*-heptadecane, the conformation looks very similar to that of *n*-decane except the average end-to-end distance and root-mean-squared radius of gyration. For example, the average C-C-C-C torsional energy per dihedral state and the average % of C-C-C-C *trans* are not much changed, and the total barrier crossings are increased but the average value per dihedral state is also not changed from *n*-decane to *n*-heptadecane (56.3/57.4). As the carbon number of *n*-alkane increases from *n*-butane to *n*-heptadecane, the total C-C LJ energy is more negative and the pressure is decreased with a large variance.

Thermodynamic properties of model II for liquid *n*-butane, *n*-decane, and *n*-heptadecane are listed in Table 4. As discussed in section II, the difference between models I and II is the inclusion of C-C bond stretching and C-C-C bond angle bending potentials. Consequently very similar results for thermodynamic properties are expected: C-C LJ energies, C-C-C-C torsional energies, end-to-end distances, and radii of gyration. Atomic temperatures and pressures show a large variance, even though the same potential parameters are

Table 5. Thermodynamic properties of model III for liquid *n*-butane, *n*-decane, and *n*-heptadecane

properties	*n*-butane	*n*-decane	*n*-heptadecane
molecular temperature (K)	291.0± 0.2	293.15± 0.39	296.0± 0.41
atomic temperature (K)	273.9± 23.8	269.38± 34.19	268.8± 43.7
pressure (atm)	47.7± 343.2	−106.7± 512.6	−206.7± 467.9
total LJ energy (kJ/mol)	−15.88± 0.06	−47.25± 0.87	−81.45± 1.34
inter C-C LJ energy	−7.33± 0.05	−20.93± 0.48	−37.30± 0.45
inter C-H LJ energy	−7.12± 0.16	−18.36± 0.36	−31.66± 0.54
inter H-H LJ energy	−0.85± 0.17	−3.18± 0.87	−2.42± 0.55
intra C-C LJ energy	−	−1.52± 0.04	−3.34± 0.08
intra C-H LJ energy	−0.23± 0.05	−2.10± 0.18	−4.37± 0.23
intra H-H LJ energy	−0.35± 0.04	−1.16± 0.17	−2.36± 0.22
C-C-C-C torsional enrgy	2.436± 0.334	2.207± 0.230	2.296± 0.21
C-C-C-H torsional energy	1.461± 0.211	1.337± 0.320	1.335± 0.29
C-C stretching energy	4.829± 0.554	11.55± 1.67	19.69± 3.29
C-H stretching energy	18.19± 1.48	30.90± 3.78	48.57± 8.34
C-C-C angle bending energy	2.321± 0.336	8.543± 1.325	15.64± 2.09
C-C-H angle bending energy	10.65± 0.93	14.85± 2.08	21.44± 3.65
H-C-H angle bending energy	18.20± 1.31	40.09± 4.62	66.60± 10.34
average % of C-C-C-C *trans*	73.39± 2.83	80.53± 7.47	77.79± 5.03
total barrier crossings T-G	169/100,000	568/100,000	1155/100,000
G-T	171/100,000	563/100,000	1159/100,000
av. end-to-end distance (nm)	0.3663± 0.0026	0.9956± 0.0130	1.5976± 0.0225
rms radius of gyration	0.1443± 0.0010	0.3377± 0.0025	0.5383± 0.0044

used except C-C bond stretching and C-C-C bond angle bending potentials. The average % of C-C-C-C *trans* are increased by 3-5% and accordingly the average end-to-end distances and root-mean-squared radii of gyration are slightly increased. The total barrier crossings of model II are not much different from model I and the average value per dihedral state is not changed from *n*-decane to *n*-heptadecane (57.0/60.6) as observed in Model I.

A detailed discussion of thermodynamic and some structural properties of model II for 14 liquid *n*-alkanes as a function of the carbon number follows. The properties of model III for liquid *n*-butane, *n*-decane, and *n*-heptadecane are listed in Table 5. As the carbon number of *n*-alkane increases, not only the total LJ energy is negatively much increased but also the intra bond stretching and bond angle bending energies are increased. However, the average % of C-C-C-C *trans*, and the C-C-C-C and C-C-C-H torsional energies are not much changed. The total barrier crossing is increased but the average value per dihedral state is not changed from *n*-decane to *n*-heptadecane (81.1/82.5) as observed in models I and II. The atomic temperatures of liquid *n*-butane, *n*-decane, and *n*-heptadecane in all the models are lower than the corresponding molecular temperature. Total LJ energies of model III are more than total C-C LJ energies of model I and II since LJ parameters are changed on considering the H atoms in the monomeric units explicitly. The pressure of the system shows a large variance like in models I and II. The average % of C-C-C-C *trans* of model III are higher than those of models I and II but the torsional energies show a small variance since the torsional energies decrease as the average % of C-C-C-C *trans* increase. The average end-to-end distances and root-mean-squared radii of gyration of model III are larger than those of models I and II due to the increase in the average % of C-C-C-C *trans*.

Some thermodynamic and structural properties of model II for 14 liquid *n*-alkanes, from *n*-butane to *n*-heptadecane, as a function of the carbon number of *n*-alkane are shown in Figures 1-3. In Figure 1, as the carbon number increases, the LJ energy of *n*-alkane is monotonically decreased (negatively increased) with a slope of −6.93 kJ/mol carbon, but the C-C bond stretching and C-C-C bond angle bending energies increase with small variance, while the average torsional energy per dihedral state is almost constant. As the number of C-C chains increases, the deviation from the equilibrium C-C bond length and C-C-C bond angle is increased due to the constraint force on the local segmental motions.

The atomic temperature and pressure of each system are shown in Figure 2. The atomic temperature increases smoothly from *n*-butane to *n*-heptane, then suddenly from *n*-heptane to *n*-octane, and saturates at 230 K. The pressure monotonically decreases to *n*-tetradecane with trace of saturation afterward.

In Figure 3, the average end-to-end distance and root-mean-squared radius of gyration are seen to increase as the carbon number increases with slopes of 0.085 and 0.028 nm/carbon, respectively. The average % of C-C-C-C *trans* increases from *n*-butane to *n*-heptane and becomes saturated at 75% as the carbon number increases further. This saturation of the average % of C-C-C-C *trans* was also observed in another computer simulation study of *n*-alkane-like models,[37] in which the average % of C-C-C-C *trans* increased from 59.6 for n (the number of carbon)=4 to 70.6 for n=8,

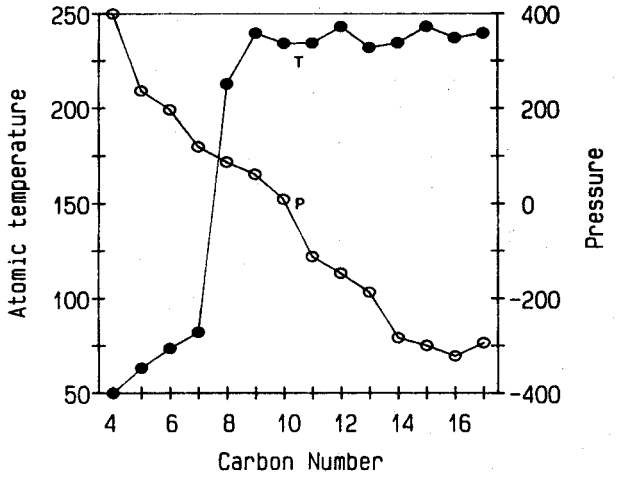

Figure 2. Atomic temperature and system pressure of model II for liquid n-alkanes as a function of carbon number.

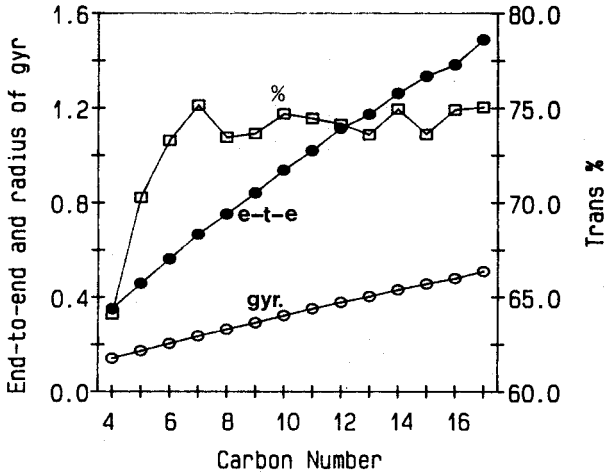

Figure 3. Root-mean-squared end-to-end distance, radius of gyration, and % of C-C-C-C *trans* of model II for liquid *n*-alkanes as a function of carbon number.

and became saturated at about 72, and showing only a small change from 71.2 for n=10 to 72.5 for n=100. The time dependent property of *trans-gauche* transition of model II for liquid *n*-alkane will be discussed in a next paper.[38]

Structural properties. The site-site radial distribution functions, g(r), of models I, II, and III for liquid *n*-alkanes are shown in Figure 4. The agreement of our results for model I of *n*-butane and *n*-decane is excellent with those of Edberg *et al.*.[10] The sharp peaks in the g(r) functions of all alkanes are due to the contribution from intramolecular sites while the smooth parts come from intermolecular sites. For example, in the case of *n*-butane - Figure 4(a), the two peaks correspond to *gauche* (G) and *trans* (T), and the third broad curve (B) corresponds to the contribution between intermolecular sites. The shaper G and T peaks in model I than those in model II are due to the rigidity of the C-C bond lengths and C-C-C bond angles of model I. These also can be seen in the cases of *n*-decane and *n*-heptadecane - Figures 4(e) and (f).

In Figures 4(b), (c), and (d), the g(r) of *n*-pentane, *n*-hexane, and *n*-heptane shows the contributions of TT, TTT, and TTTT at $r^*=1.27$, 1.61, and 1.91, respectively, where $r^*=r/\sigma$, and the TG (or GT) peak becomes clear at about $r^*=1.1$ as the number of carbon increases from *n*-pentane to *n*-heptane, although the exact end-to-end distance of the TG conformation is $r^*=1.04$. This is because site-site distances for T and continuous T conformations are always less than or equal to a maximum extension which corresponds to all of the included dihedral angles being exctly zero, and those for the conformations with at least one G may be generally greater than the exact end-to-end distances with the exact dihedral angles being zero or 180 since the G conformation in *n*-butane has a distance greater than or equal to a minimum distance which corresponds to the dihedral angle being exactly 180.

As the number of carbon increases, the peaks are more complicated and higher, but the trend is unchanged from *n*-octane to *n*-heptadecane. In Figures 4 (e) and (f) for *n*-decane and *n*-heptadecane, the two sharp peaks at about $r^*=1.3$ and 1.45 between TT and TTT conformations represent the contributions of TTG (or GTT) and TGT conformations, in which the exact distances are $r^*=1.23$ and 1.43, respectively. Another sharp peak at about $r^*=1.8$ between TTT and TTTT conformations is due to the contributions of TTTG and TGTG (or GTGT) in which the exact distance is $r^*=1.60$. The exact distance of the TTTTT contribution at about $r^*=2.2$ in Figure 4(f) is $r^*=2.24$.

In Figure 4(g) we show the radial distribution functions of C-C site-site of model III for *n*-butane, *n*-decane, and *n*-heptadecane. As the number of carbon increases, the peaks become higher, even though there is a slight difference between those functions of *n*-decane and *n*-heptadecane. Comparing with models I and II for the three *n*-alkanes, model I has the highest peaks due to the rigidity of C-C bond lengths and C-C-C bond angles, and model III has higher peaks than those of model II except the first G peak. In all the three *n*-alkanes, the first G peaks of model III shift to the larger r^* by 0.04 σ and the broad curves which correspond to the contribution between intermolecular sites (B in Figure 4(a)) are much different from that of models I and II.

In order to see the contribution between intermolecular sites in more detail, we show the inter C-C site-site radial distribution functions of models II and III for *n*-butane and *n*-decane in Figure 4(h). The functions for *n*-heptadecane are omitted because they are very similar to those for *n*-decane, and those of model I are also omitted because of similarity to those of model II. This kind of radial distribution function already appeared in the MD study of liquid hydrocarbons (methane to hexane).[39] Both radial distribution functions of model III show almost the same shift to the smaller r^* over the whole range of r^* except short coincidence with those of model II before the peaks. It is worth noting that this trend is exactly the same in both functions of model III for *n*-butane and *n*-decane (also *n*-heptadecane) in comparing with model II. This implies that the thermodynamics properties of model III may be not much different from those of models I and II, but the structural properties such as g(r), the average end-to-end distance and root-mean-squared radius of gyration are very different.

In Figures 5 and 6, we have shown the average end-to-

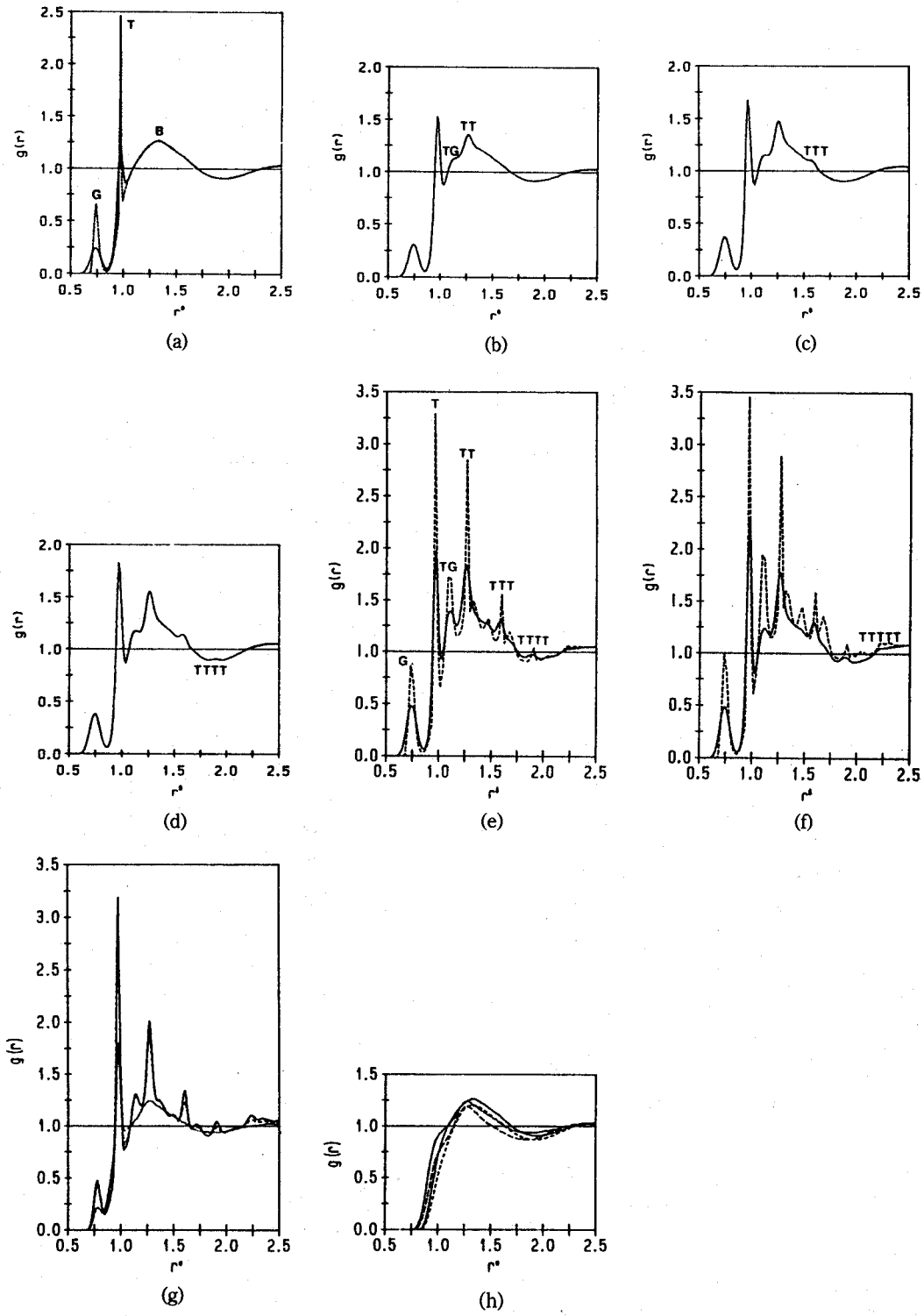

Figure 4. Site-site radial distribution functions of models I, II, and III for liquid *n*-alkanes, $r^*=r/\sigma$. (a) *n*-butane, (b) *n*-pentane, (c) *n*-hexane, (d) *n*-heptane, (e) *n*-decane, and (f) *n*-heptadecane of models I (---) and II(—), (g) *n*-butane (···), *n*-decane (---), and *n*-heptadecane (—) model III, and (h) inter C-C site-site radial distributions functions of model II for *n*-butane (—) and *n*-decane (---), and model III for *n*-butane (···) and *n*-decane (---).

end distance distribution functions for model II of all liquid *n*-alkanes as a function of r* and those for models I, II, and III of *n*-butane, *n*-decane, and *n*-heptadecane. In the low carbon number alkanes, the contribution of *trans* conformation is dominant in the end-to-end distance distribution. For example, for *n*-butane, the lower peak at about $r^*=0.7$ is from the *gauche*(G) conformation at the exact end-to-end distance $r^*=0.65$ and the higher peak at about $r^*=1.0$ is from the *trans*(T) at the exact end-to-end distance $r^*=0.98$. For *n*-pentane, the lower peak at about $r^*=1.0$ is contributed

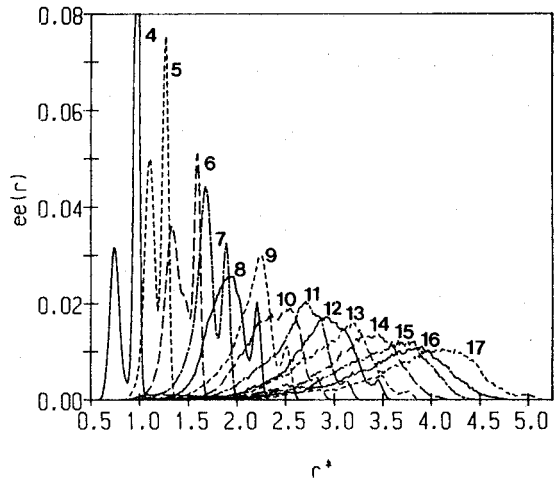

Figure 5. Average end-to-end distance distribution of model II for liquid *n*-alkanes. The number indicates the number of carbon in *n*-alkane. The peak of number 4 reaches upto 0.1416.

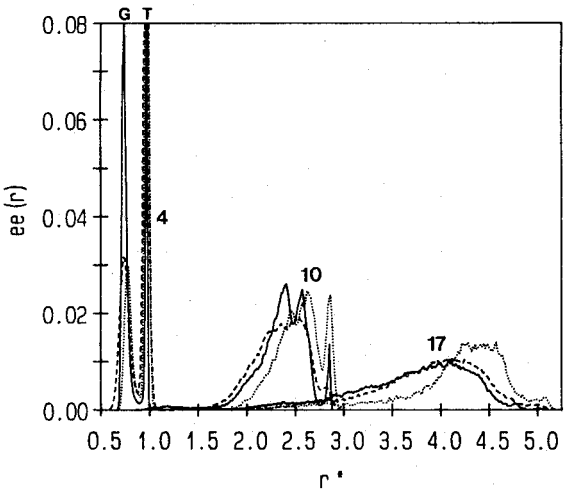

Figure 6. Average end-to-end distance distribution of models I(—), II(---), and (···) III for liquid *n*-butane, *n*-decane, and *n*-heptadecane. The number indicates the number of carbon in *n*-alkane. The peak of number 4 reaches up to 0.0824 (G) and 0.4761 (T) for model I and 0.2162 for model III.

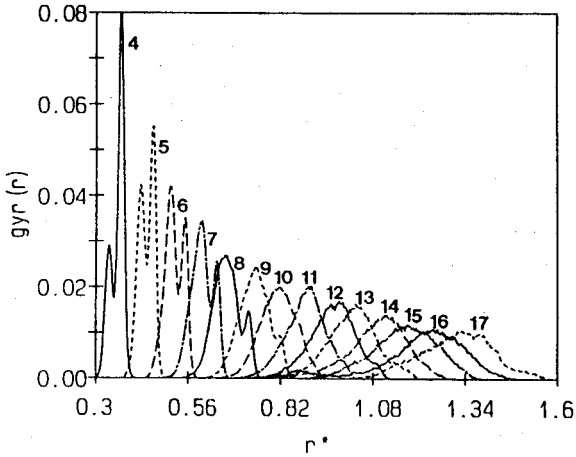

Figure 7. Root-mean-squared radius of gyration distribution of model II for liquid *n*-alkanes. The number indicates the number of carbon in *n*-alkane. The peak of number 4 reaches upto 0.0835.

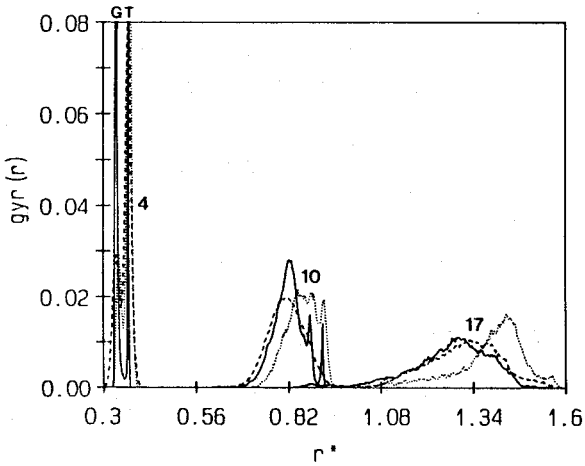

Figure 8. Root-mean-squared radius of gyration distribution of models I(—), II(---), and III(···) for liquid *n*-butane, *n*-decane, and *n*-heptadecane. The number indicates the number of carbon in *n*-alkane. The peak of number 4 reaches up to 0.1178 (G) and 0.5285 (T) for model I and 0.1308 for model III.

by the GT (or TG) conformation at the exact distance r*= 1.04 and the higher peak at about r*=1.25 is from the TT conformation at an end-to-end distance r*=1.27. Likewise, for *n*-hexane, the lower peak at about r*=1.3 is due to the TTG (or GTT) of the exact end-to-end distance r*=1.23, the higher peak at about r*=1.6 comes from the TTT conformation exactly at r*=1.61. The dent between these two peaks at about r*=1.4 is due to the TGT conformation at r*=1.43.

As the carbon number increases, the contribution of *trans* conformations decreases. For example, for *n*-heptane, the higher peak at about r*=1.7 is contributed by the TTTG and TGTG (or GTGT) conformations at the exact end-to-end distance r*=1.60 and the lower peak at about r*=1.9 by the TTTT of the exact end-to-end distance r*=1.91. In the high carbon number alkanes, the contribution of *trans* conformation is disappeared.

For model III in Figure 6, the sharp peaks of *n*-butane are due to the rigidity of C-C bond lengths and C-C-C bond angles. The population of gauche (G) looks more than that of *trans*(T), but it is not true since the average % of C-C-C-C *trans* of model I for *n*-butane is 60.02 from Table 3. In models II and III, the peaks become broader and the shift of the first G peak of model III for *n*-butane is also seen. For *n*-decane and *n*-heptadecane, model I has more sharp peaks than model II, and model III shows considerable shifts of structural peaks to the larger r*, especially in the case of *n*-heptadecane, which shows the very difference of structures of model III from models I and II.

The distributions of root-mean-squared radii of gyration for liquid *n*-alkanes are displayed in Figs. 7 and 8 and has the same features as those of the average end-to-end distance: in the low carbon number alkanes, the contribution of

trans conformation is dominant, but as the carbon number increases, it decreases, and in the high carbon number alkanes, it disappears. However, the disappearance of contribution of *trans* conformation occurs at a lower number of carbon atoms here than in the distribution of end-to-end distance.

For model III in Figure 8, the overall trends of the root-mean-squared radii of gyration for *n*-butane, *n*-decane, and *n*-heptadecane are very similar to the average end-to-end distances with the shift of the first G peak of model III from models I and II for *n*-butane. The structural difference of model III appears more clearly for *n*-heptadecane.

Conclusion

We have presented the results of thermodynamic and structural properties from MD simulation of liquid *n*-alkanes. Excellent agreement of the results of model I for *n*-butane from different MD algorithms, ours and those of Edberg *et al.*,[10] confirms the validity of our whole set of MD simulations of model II for 14 liquid *n*-alkanes and of models I and III for liquid *n*-butane, *n*-decane, and *n*-heptadecane. The thermodynamic and structural properties of model I and II are very similar to each other and the thermodynamic properties of model III for the three *n*-alkanes are not much different from those of models I and II. However, the structural properties of model III are very different from those of model I and II as seen from the radial distribution functions, the average end-to-end distances, and the root-mean-squared radii of gyration.

Acknowledgment. This work was supported by Basic Science Research Institute Program, Ministry of Education (BSRI-94-3414). S. H. L. thanks the Korea Institute of Sciences and Technology for access to the Cray-C90 super computer and J. C. R. acknowledges the facilities provided by the Computer and Data Processing Services (CAPS) at the University of Maine.

References

1. Morrison, R. T.; Boyd, R. N. *Organic Chemistry*; 5th ed.; Allyn and Bacon: Boston, 1987.
2. Bird, R. B.; Hassager, O.; Amstrong, R. C.; Curtiss, C. F. *Dynamics of Polymeric Liquids* Vol. 2: *Kinetic Theory* 2nd ed; Wiley: New York, 1977.
3. Rudisill, J. W.; Cummings, P. T. *Rheol. Acta* **1991**, *30*, 33.
4. Rudisill, J. W.; Cummings, P. T. *J. Non-Newton. Fluid Mech.* **1992**, *41*, 275.
5. Rudisill, J. W.; Cummings, P. T. *Fluid Phase Equil.* **1993**, *88*, 99.
6. Rudisill, J. W.; Fetsko, S. W.; Cummings, P. T. *Comput. Polymer Science* **1993**, *3*, 23.
7. Ryckaert, J. P.; Bellemans, A. *Discuss. Faraday Soc.* **1978**, *66*, 95.
8. Ryckaert, J. P.; Ciccotti, G.; Berendsen, H. J. C. *J. Comput. Phys.* **1977**, *23*, 327.
9. Wielopolsky, P. A.; Smith, E. R. *J. Chem. Phys.* **1986**, *84*, 6940.
10. Edberg, R.; Evans, D. J.; Morriss, G. P. *J. Chem. Phys.* **1986**, *84*, 6933.
11. Baranyai, A.; Evans, D. J. *Mol. Phys.* **1990**, *70*, 53.
12. Edberg, R.; Morriss, G. P.; Evans, D. J. *J. Chem. Phys.* **1987**, *86*, 4555.
13. Morriss, G. P.; Daivis, P. J.; Evans, D. J. *J. Chem. Phys.* **1991**, *94*, 7420.
14. Daivis, P. J.; Evans, D. J.; Morriss, G. P. *J. Chem. Phys.* **1992**, *97*, 616.
15. Daivis, P. J.; Evans, D. J. *J. Chem. Phys.* **1994**, *100*, 541.
16. Andersen, H. C.; Chandler, D.; Weeks, J. D. *J. Chem. Phys.* **1972**, *56*, 3881.
17. Andersen, H. C.; Chandler, D.; Weeks, J. D. *Adv. Chem. Phys.* **1976**, *34*, 105.
18. Rowley, R. L.; Ely, J. F. *Mol. Phys.* **1991**, *72*, 831.
19. Rowley, R. L.; Ely, J. F. *Mol. Phys.* **1992**, *75*, 713.
20. Chynoweth, S.; Klomp, U. C.; Scales, L. E. *Comput. Phys. Commun.* **1991**, *62*, 297.
21. Chynoweth, S.; Klomp, U. C.; Michopoulos, Y. *J. Chem. Phys.* **1991**, *95*, 3024.
22. Berker, A.; Chynoweth, S.; Klomp, U. C.; Michopoulos, Y. *J. Chem. Soc. Faraday Trans.* **1992**, *88*, 1719.
23. Toxvaerd, S. *J. Chem. Phys.* **1990**, *93*, 4290.
24. Muller-Plathe, F. *J. Chem. Phys.* **1991**, *94*, 3192.
25. Muller-Plathe, F. *J. Chem. Phys.* **1992**, *96*, 3200.
26. Muller-Plathe, F.; Rogers, S. C.; van Gunsteren, W. F. *Chem. Phys. Lett.* **1992**, *199*, 237.
27. Muller-Plathe, F.; Rogers, S. C.; van Gunsteren, W. F. *Macromolecules* **1992**, *67*, 22.
28. Muller-Plathe, F.; Rogers, S. C.; van Gunsteren, W. F. *J. Chem. Phys.* **1993**, *98*, 9895.
29. Gusev, A. A.; Muller-Plathe, F.; van Gunsteren, W. F.; Suter, U. W. *Dynamics of small molecules in bulk polymers* in Atomistic Modeling of Physical Properties; Monnerie, L.; Suter, U. W. Ed.; Springer-Verlag.; Berlin, 1994.
30. Lee, S. H.; Cummings, P. T. *Mol. Sim.* **1996**, *16*, 229.
31. (a) Evans, D. J.; Hoover, W. G.; Failor, B. H.; Moran, B.; Ladd, A. *J. C. Phys. Rev.* **1983**, *A28*, 1016. (b) Simmons, A. D.; Cummings, P. T. *Chem. Phys. Lett.* **1986**, *129*, 92.
32. Allen, M. P.; Tildesley, D. J. *Computer Simulation of Liquids*; Oxford: Oxford Univ. Press., 1987.
33. Andersen, H. C. *J. Comp. Phys.* **1983**, *52*, 24.
34. White, D. N. J.; Boville, M. J. *J. Chem. Soc. Perkin Trans.* **1977**, *2*, 1610.
35. Gear, C. W. *Numerical Initial Value Problems in Ordinary Differential Equation*; Englewood Cliffs NJ; Prentice-Hall, 1971.
36. Ryckaert, J. P.; McDonald, I. R.; Klein, K. L. *Mol. Phys.* **1989**, *67*, 957.
37. Brown, D.; Clarke, J. H. R.; Okuda, M.; Yamazaki, T. *J. Chem. Phys.* **1994**, *100*, 1684.
38. Lee, S. H.; Lee, H.; Pak, H.; Rasaiah, J. C. *in preparation.*.
39. Im, W.; Won, Y. *Bull. Kor. Chem. Soc.* **1994**, *15*, 852.